crystals

MDPI

Article

Synthesis, Crystal Structures, and Photoluminescent Properties of Two Supramolecular Architectures Based on Difunctional Ligands Containing Imidazolyl and Carboxyl Groups

Mei-An Zhu, Xing-Zhe Guo, Shan-Shan Shi and Shui-Sheng Chen *

College of Chemistry & Chemical Engineering, Fuyang Normal University, Fuyang 236041, China; zhumeian2017@163.com (M.-A.Z.); njncwater@163.com (X.-Z.G.); shishanshanshan@126.com (S.-S.S.)
* Correspondence: fyuniv@163.com; Tel.: +86-558-2595836

Academic Editor: Shujun Zhang
Received: 13 June 2017; Accepted: 21 July 2017; Published: 23 July 2017

Abstract: Two new supramolecular architectures, namely, $[Cd(L_1)_2(H_2O)]_n$ (**1**) and $[Ni(L_2)_2(H_2O)]_n$ (**2**), were synthesized by the reaction of corresponding metal salts of $CdCl_2 \cdot 2.5H_2O$ and $NiCl_2 \cdot 6H_2O$ with 2-(1*H*-imidazol-4-yl)benzoic acid (**HL_1**) and 3-(1*H*-imidazol-4-yl)benzoic acid (**HL_2**) respectively, and characterized by single-crystal X-ray diffraction, IR spectroscopy, elemental analysis and powder X-ray diffraction (PXRD). Both HL_1 and HL_2 ligands are deprotonated to be L_1^- and L_2^- anions that coordinate with Cd(II) and Ni(II) atoms to form two-dimensional (2D) layer structure. Topologically, complex **1** is a 2D network with (4, 4) **sql** topology, while **2** is a typical 6^3-**hcb** topology net. Complex **1** exhibits intense light blue emission in the solid state at room temperature.

Keywords: supramolecular architectures; noncovalent interactions; photoluminescent property

1. Introduction

The rational design and construction of metal-organic frameworks (MOFs) has become an expanding research topic in the fields of supramolecular chemistry and crystal engineering not only because of their intriguing molecular architectures and intricate topologies but also their promising applications in various areas in fluorescence, gas adsorption, separation, ion exchange, magnetic properties, catalysis, and so on [1–6]. Because the complexes incorporate metallic centers and bridging organic linkers, therefore, it is important to design suitable organic ligands and choose metallic centers to assemble desirable frameworks with specific structures and functions.

Due to their favorable coordination abilities for the N or O donor atoms, the organic linkers incorporating N-heterocyclic bridging or carboxyl groups ligands are extensively applied to construct coordination polymers and have made great progress in the field of crystal engineering [7,8]. The N-heterocyclic bridging ligands include imidazole, triazole, tetrazole, and pyridine or its analogues such as pyridazine, tetrazine, triazine, and pyrazine moieties [9–12]. In our previous studies, we have elaborately designed the series of novel 4-imidazole ligands with flexible coordination modes, and successfully employed the ligands to construct porous frameworks based on the 4-imidazolate-metal building units [13–15], and the porous frameworks exhibit favorable gas adsorption properties. Taking the various coordination modes of carboxyl group into consideration, we have further carried out studies to design another type of novel difunctional ligand containing 4-imidazolyl group and carboxyl group [16]. Furthermore, the novel organic ligand was applied to construct two series Cu(II) and Cd(II) coordination polymers based on its flexible coordination modes. It should be noted that difunctional groups occupy the 1- and 4-position of benzene ring respectively,

and as a result, the ligand often act as linear 2-connected node exhibited in resulting coordination polymers. As an extension of our previous work, we have designed two isomers of 4-(1*H*-imidazol-4-yl)benzoic acid [16] and synthesized two new organic ligands-2-(1*H*-imidazol-4-yl)benzoic acid (**HL_1**) and 3-(1*H*-imidazol-4-yl)benzoic acid (**HL_2**). Here, we report the synthesis and crystal structures of two new coordination polymers of $[Cd(L_1)_2(H_2O)_2]_n$ (**1**) and $[Ni(L_2)_2(H_2O)]_n$ (**2**) obtained by the reaction of **HL_1** and **HL_2** with corresponding metal salts under hydrothermal condition.

2. Results and Discussion

*2.1. Structural Description of $[Cd(L_1)_2(H_2O)]_n$ (**1**)*

The X-ray single-crystal structural analysis reveals that complex **1** crystallizes in monoclinic *C*2/*c* space group, and the asymmetric unit has a half molecule of $[Cd(L_1)_2(H_2O)]$, namely, a Cd(II) atom sitting on a special position with a half of occupancy, one L_1^- ligand, and a half of coordinated water molecule. As shown in Figure 1, the Cd1 center with O_5N_2 pentagonal bipyramid geometry is coordinated by two pairs of oxygen atoms (O(1A), O(2A) and O(1B), O(2B)) of two chelating carboxylate groups from two distinct L_1^- ligands [17,18], another oxygen atom from coordinated water molecule (O3) in the basal plane and two nitrogen atoms (N1, N1C) from other two L_1^- ligands in apical positions. The bond lengths of Cd–O (2.298–2.453(7) Å) and Cd–N (2.255(8) Å) are in line with those of the reported compounds consisting of O–Cd–N segments, and the coordination angles around Cd1 are in the range of 53.5(2)∼173.9(5)° (Table 1).

The organic molecule of HL_1 was deprotonated to L_1^- and act as a μ_2-bridge to link two Cd(II) atoms using the imidazolyl and carboxyl coordination groups respectively. It should be noteworthy that these difunctional groups occupy the adjacent positions and result in serious steric effect, which promote these two group distortedly twist from the benzene plane. That is, the aromatic rings of phenyl and imidazolyl rings are nearly perpendicular, with the dihedral angle of 84.99° while the plane of carboxyl group twists from benzene ring with 52.367° respectively. In this sense, the HL_1 ligand is quite different from the ligand of 4-(1*H*-imidazol-4-yl)benzoic acid reported in our previous study, that the aromatic groups often are coplanar due to lack of steric hindrance.

Each L_1^- ligand acts as 2-connector to link two Cd(II) atoms, while each Cd(II) atom in return connects four different L^- ligands. In this connection, the Cd(II) atoms are linked to form a two-dimensional (2D) network along the *ab* plane (Figure 2). Topologically, the 2D layer is (4, 4) net, where L_1^- ligand and Cd(II) atom act as 2- and 4-connector respectively, and the lateral Cd···Cd distances are 7.49 Å, and the diagonal Cd···Cd distances are 6.27 and 13.61 Å. It should be noted that numerous intermolecular π–π and C-H···π interactions exist among the aromatic rings, as shown in Figure 3. The benzene rings of the L_1^- ligands between the adjacent 2D layers are parallel and are separated by a centroid-centroid distance of 3.94 Å and C-H···π distance of 3.32 Å [7,19]. The non-classic weak π–π and C-H···π interactions further link the 2D layers into three-dimensional (3D) supramolecular polymer (Figure 3).

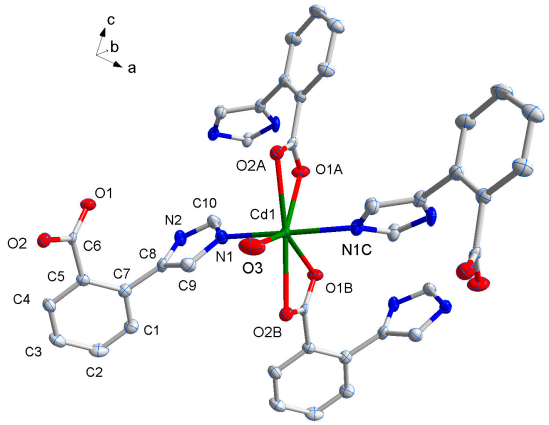

Figure 1. The coordination environment of Cd(II) ion in **1** with the ellipsoids drawn at the 30% probability level. Symmetry codes: A 1.5 − x, 0.5 + y, 0.5 − z, B 0.5 + x, 0.5 + y, z, C 2 − x, y, 0.5 − z.

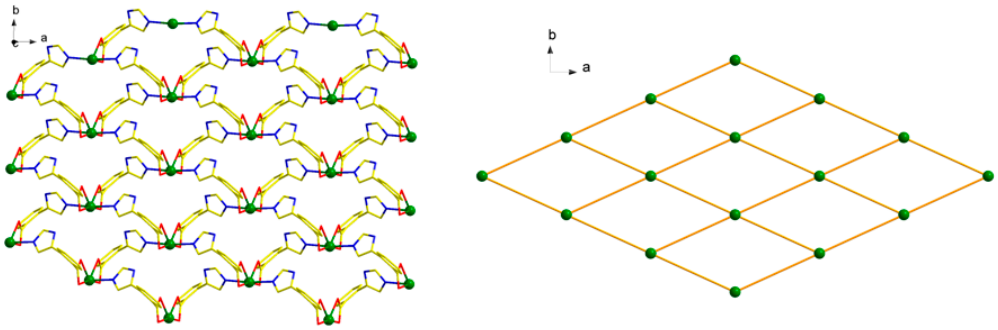

Figure 2. 2D layered structure (left) and 2D (4, 4) **sql** layered network of **1** (right).

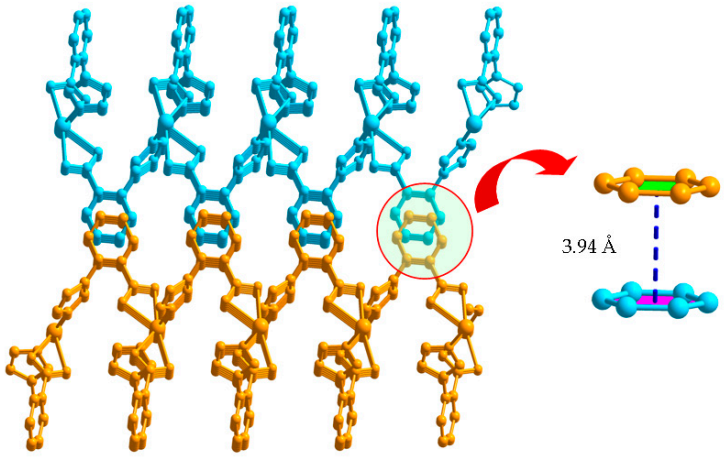

Figure 3. 3D supramolecular network structure of **1** linked by π···π interactions.

*2.2. Structural Description of [Ni(L$_2$)$_2$(H$_2$O)]$_n$ (**2**)*

Compound **2** crystallizes in the monoclinic space group P2$_1$/c, and the asymmetric unit contains one unique Ni(II) atom, two L$_2^-$ ligands, and one coordinated water molecule. As shown in Figure 4, the Ni1 has a distorted octahedral environment, in which the equatorial plane contains O3, O4 atoms of one chelating carboxylate groups from one L$_2^-$ ligand, and N3A, O2B from other two distinct L$_2^-$ ligands, and the atoms N1 and O5 from L$^-$ ligand and coordinated water molecule occupy the axial positions with an N1−Ni1−O5 angle of 175.19(5)° (Table 1). Two carboxyl groups from different

L_2^- ligand adopt μ_1-η^1:η^0-monodentate and μ_1-η^1:η^1-chelating coordination modes to coordinate with Ni(II) atoms while the imidazolyl groups both employ the external N atoms to link Ni(II) atoms. As a result, two different L_2^- both act as μ_2-bridge to link two Ni(II) atoms, and in return, each Ni(II) atom link other three Ni(II) atoms by the L_2^- ligand. Topologically, L_2^- ligands bridge the Ni(II) atoms to form a 2D layer with 6^3-**hcb** topology where the Ni(II) atom and L^- ligand act as 3- and 2-connected nodes respectively (Figure 5). Compared with HL_1 ligand, the dihedral angle between two different imidazolyl groups and benzene rings from HL_2 are 21.126 and 16.304°, not twisting distortedly as **1**, because the imidazolyl and carboxyl groups occupy the meta-position, avoiding the steric hindrance.

There exist weak interactions including rich hydrogen bond and π−π stacking interactions. Noticeably, the NH or N atom of imidazolyl groups and carboxyl group can act as hydrogen bonding donor or acceptor, which benefits the construction of supramolecular structures. In **2**, it can be seen clearly that the N−H···O, O−H···O hydrogen bonds (N(4)···O(1) 2.833(18) Å, N(4)–H(4)···O(1) 144°; O(5)···O(4) 2.781(16) Å, O(5)–H(5B)···O(4) 176°) connect the adjacent 2D layers to produce 3D supramolecular polymer (Figure 6, Table 2). Particularly, two benzene rings of the L_2^- ligands between the adjacent 2D layers are nearly parallel with a dihedral angle of 3.16° and are separated by a centroid−centroid distance of 3.56 Å, indicating the presence of strong π−π stacking interactions (Figure 6). Therefore, the overall framework of **2** is a 3D supramolecular polymer by rich N−H···O and O−H···O hydrogen bonds and strong π–π stacking interactions. The total void value of the channel is estimated to be 76.5 $Å^3$, 4.0 % of the total crystal volume of 1910.9 $Å^3$.

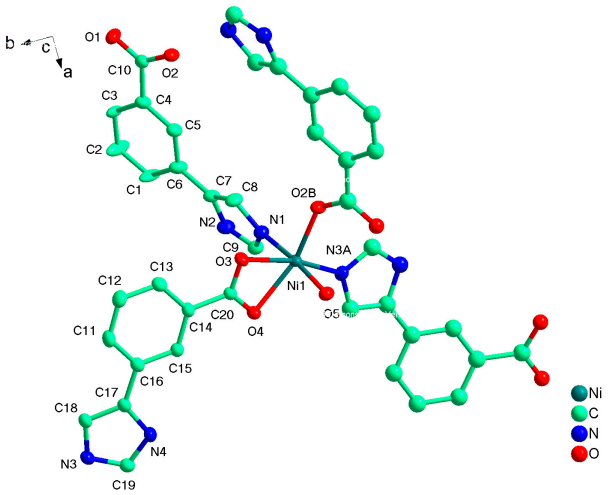

Figure 4. The coordination environment of Ni(II) ion in **2** with the ellipsoids drawn at the 30% probability level. Symmetry code: A 1 − x, 2 − y, 1 − z, B 2 − x, 0.5 + y, 1.5 − z.

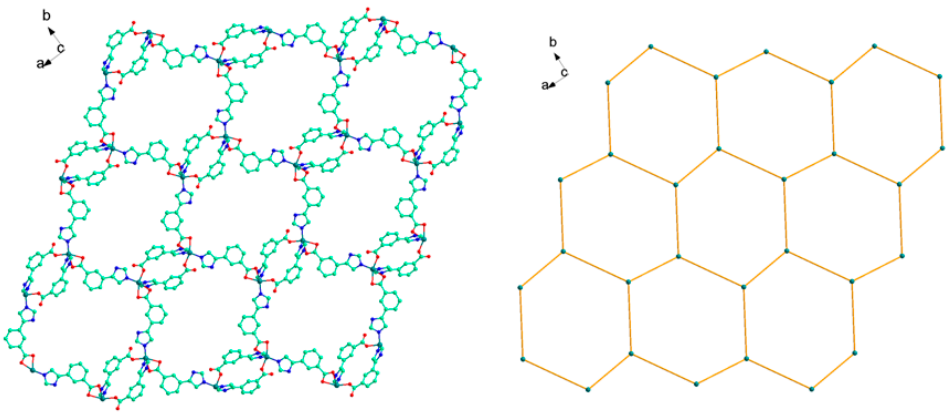

Figure 5. The 2D network structure (left) and the representation of 6^3-**hcb** framework of **2** (right).

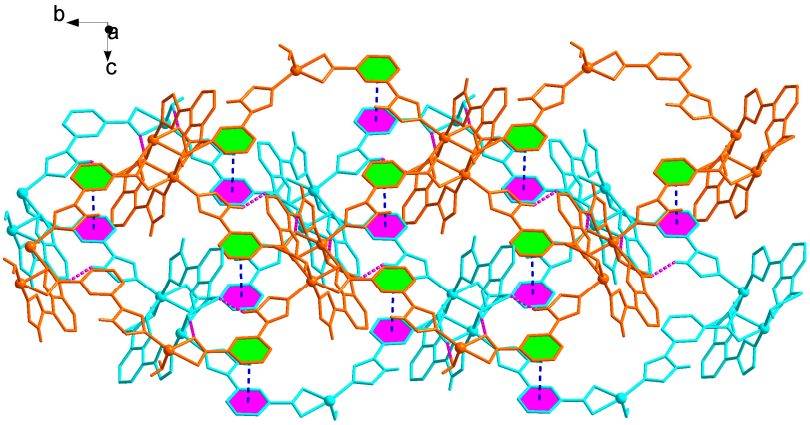

Figure 6. 3D supramolecular network structure of **2** linked by hydrogen bonds and π–π stacking interactions highlighted by pink and blue dotted line, respectively.

Table 1. Selected bond lengths (Å) and bond angles (°) for **1** and **2**.

Bond	*d*	Bond	*d*
	1		
Cd(1)-N(1)	2.255(8)	Cd(1)-O(3)	2.298(11)
Cd(1)-O(1)^{ii}	2.438(8)	Cd(1)-O(2)^{ii}	2.453(7)
	2		
Ni(1)-N(1)	2.0654(13)	Ni(1)-N(3)^{v}	2.0252(13)
Ni(1)-O(2)^{iv}	2.0123(11)	Ni(1)-O(3)	2.1211(11)
Ni(1)-O(5)	2.1475(12)	Ni(1)-O(4)	2.1541(10)
Angle	ω	**Angle**	ω
	1		
N(1)-Cd(1)-N(1)^{i}	173.9(5)	N(1)-Cd(1)-O(3)	93.0(2)
N(1)-Cd(1)-O(1)^{ii}	88.3(3)	O(3)-Cd(1)-O(1)^{ii}	136.76(17)
(1)^{ii}-Cd(1)-O(1)^{iii}	86.5(3)	N(1)-Cd(1)-O(2)^{ii}	86.0(3)
N(1)-Cd(1)-O(2)^{iii}	94.7(3)	O(3)-Cd(1)-O(2)^{ii}	83.46(15)
O(1)^{ii}-Cd(1)-O(2)^{ii}	53.5(2)	O(1)^{iii}-Cd(1)-O(2)^{ii}	139.5(2)
O(2)^{ii}-Cd(1)-O(2)^{iii}	166.9(3)		
	2		
O(2)^{iv}-Ni(1)-N(3)^{v}	97.46(5)	O(2)^{iv}-Ni(1)-N(1)	94.27(5)
N(3)^{v}-Ni(1)-N(1)	91.25(5)	O(2)^{iv}-Ni(1)-O(3)	94.49(4)
N(3)^{v}-Ni(1)-O(3)	168.06(5)	N(1)-Ni(1)-O(3)	87.95(5)
O(2)^{iv}-Ni(1)-O(5)	89.39(5)	N(3)^{v}-Ni(1)-O(5)	91.36(5)
N(1)-Ni(1)-O(5)	175.19(5)	O(3)-Ni(1)-O(5)	88.66(4)
O(2)^{iv}-Ni(1)-O(4)	155.91(4)	N(3)^{v}-Ni(1)-O(4)	106.31(5)
N(1)-Ni(1)-O(4)	89.15(5)	O(3)-Ni(1)-O(4)	61.77(4)
O(5)-Ni(1)-O(4)	86.24(4)		

Symmetry codes: (i) −x + 2,y,−z + 1/2; (ii) *x* + 1/2,*y* + 1/2,*z*; (iii) −*x* + 3/2,*y* + 1/2,− *z*+ 1/2; (iv) −*x*,−*y* + 1,−*z* + 1; (v) −*x* + 1,*y* − 1/2, −*z* + 3/2.

Table 2. Hydrogen bond lengths (Å) and bond angles **(°)** for **1** and **2**.

D–H···A	d(D–H)	d(H···A)	d(D···A)	∠DHA
		1		
N(2)–H(2)···O(2)^{i}	0.86	1.99	2.83(11)	166
		2		
N(2)–H(2A)···O(3)^{ii}	0.86	2.07	2.89(17)	157
N(4)–H(4)···O(1)^{iii}	0.86	2.09	2.83(18)	144
O(5)–H(5A)···O(1)^{iv}	0.82	2.00	2.73(16)	147
O(5)–H(5B)···O(4)^{v}	0.83	1.96	2.78(16)	176(2)
C(5)–H(5)···O(2)	0.93	2.40	2.73(18)	100

Symmetry code: (i) *x*,1 + *y*,*z*; (ii) *x*,*y*,1 + *z*; (iii) 1 + *x*,*y*,*z*; (iv) *x*,1 − *y*,1 − *z*; (v) 1 − *x*,1 − *y*,1 − *z*.

2.3. Thermal Analysis and Powder X-ray Diffraction Analysis

The thermal stability of complexes **1** and **2** were examined by thermogravimetric analysis (TGA) to ascertain the stability of supramolecular architectures in the N_2 atmosphere from 25–700 °C, and the result is shown in Figure 7. The complex 1 shows a weight loss of 3.50% in the temperature range of 100–125 °C, corresponding to the release of coordinated water molecules (calc. 3.57%), and the decomposition of the residue occurred at 330 °C. The first weight loss of 3.83% around 85 °C indicates the exclusion of coordinated water molecules (calc. 3.99%) for **2**, and the residue is stable up to 325 °C. Powder XRD experiment was carried out to confirm the phase purity of bulk sample, and the experimental pattern of the as-synthesized sample can be considered comparable to the corresponding simulated one, indicating the phase purity of the sample (Figure 8).

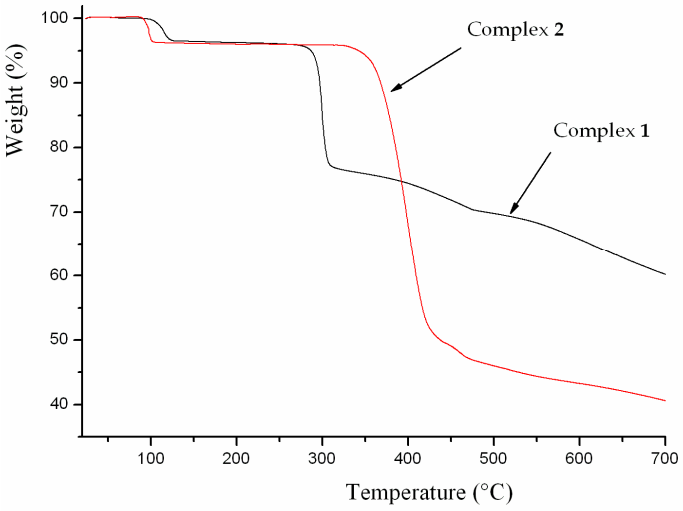

Figure 7. Thermal analysis curve of the complexes **1** and **2**.

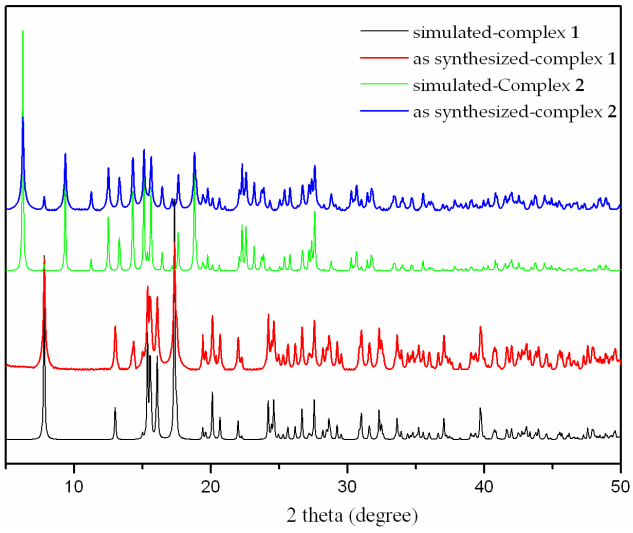

Figure 8. The X-ray powder diffraction of the complexes **1** and **2**.

2.4. Photoluminescent Property

Considering that coordination polymers with d^{10} closed-shell metal center and aromatic-containing system may exhibit excellent fluorescence properties and serve as good candidates for potential applications as photoactive materials, we investigate the solid-state fluorescence property of complex **1** as

well as the HL_1 ligand at room temperature [20–22]. The free HL_1 ligand shows emission band at 433 nm upon excitation at 407 nm, which may be attributed to $\pi^* \rightarrow \pi$ transition of the intraligands [23,24], while the complex **1** exhibits light blue emission with maximum at 455 nm upon excitation at 399 nm as depicted in Figure 9. By contrast with the free ligand, the emission bands of complex **1** are 22 nm red-shifted. Such board emission bands may be tentatively assigned to ligand-to-metal charge transfer (LMCT) [25,26].

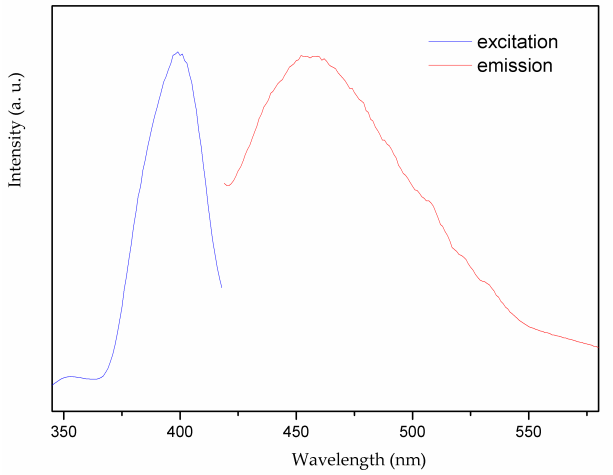

Figure 9. Solid-state photoluminescent spectra of **1** at room temperature.

3. Experimental Section

3.1. Materials and Instrumentation

All the commercially available chemicals and solvents were of reagent grade and used as received without further purification. Elemental analyses were performed on a Perkin-Elmer 240C Elemental Analyzer (PerkinElmer, Waltham, MA, USA). IR spectra were recorded on a Bruker Vector 22 FT-IR spectrophotometer (Instrument Inc., Karlsruhe, Germany) using KBr pellets. Thermogravimetric analyses (TGA) were performed on a simultaneous SDT 2960 thermal analyzer (Thermal Analysis Instrument Inc., New Castle, DE, USA) under nitrogen with a heating rate of 10 °C min^{-1}. Power X-ray diffraction (PXRD) patterns were measured on a Shimadzu XRD-6000 X-ray diffractometer (Shimadzu Corporation, Kyoto, Japan) with Cu$K\alpha$ (λ = 1.5418 Å) radiation at room temperature. The fluorescent spectra were measured using a Perkin Elmer LS-55B fluorescence spectrometer (PerkinElmer, Billerica, MA, USA).

*3.2. Synthesis of $[Cd(L_1)_2(H_2O)]_n$ (**1**)*

Reaction mixture of HL_1 (0.021 g, 0.1 mmol), $CdCl_2 \cdot 2.5H_2O$ (0.0228 g, 0.1 mmol) and 10 mL H_2O was adjusted to pH = 7 with 0.5 mol L^{-1} NaOH solution. The mixture was then sealed in a 20 mL Teflon-lined stainless steel container and heated at 120 °C for 48 h. After cooling to the room temperature, colorless block crystals of **1** were collected with a yield of 82% by filtration and washed with ethanol and water for several times. Anal. Calcd. (%) for $C_{20}H_{16}N_4O_5Cd$: C, 49.59; H, 3.19; N, 11.10. Found (%): C, 49.42; H, 3.31; N, 11.22. IR(KBr): 3665∼2640 (m), 1602 (s), 1529 (s), 1402(s), 1190 (w), 1131 (m), 1090 (s), 948 (m), 849 (m), 788 (m), 699 (w), 648 (m), 502 (m) cm^{-1}.

*3.3. Synthesis of $[Ni(L_2)_2(H_2O)]_n$ (**2**)*

Complex **2** was obtained by the same procedure used for preparation of **1** except that the $CdCl_2 \cdot 2.5H_2O$ and **HL_1** were replaced by $NiCl_2 \cdot 6H_2O$ (0.024 g, 0.1 mmol) and **HL_2** respectively. Green block crystals of **2** were collected in 78% yield. Anal. Calcd. (%) for $C_{20}H_{16}N_4O_5Ni$: C, 53.26; H,

3.58; N, 12.42. Found (%): C, 53.11; H, 3.54; N, 12.28. IR(KBr): 3635∼2360 (m), 1586 (s), 1551 (s), 1368 (s), 1313 (w), 1231 (m), 1169 (m), 1068 (w), 969 (m), 842 (m), 779 (s), 709 (m), 630 (m), 590 (m), 522 (w) cm^{-1}.

3.4. Crystal Structure Determination

The single crystal data of $[Cd(L_1)_2(H_2O)]_n$ (**1**) and $[Ni(L_2)_2(H_2O)]_n$ (**2**) were collected on a Bruker Smart APEX CCD diffractometer (Bruker, Karlsruhe, Germany) with graphite-monochromated MoKα radiation (λ = 0.71073 Å) at 293(2) K. The structure was solved by direct method and refined by full-matrix least squares on F^2 using the SHELX-97 program [27]. The hydrogen atoms were generated geometrically except that H5B of water molecule in **1** was found at reasonable positions in the differential Fourier map and located there. The crystallographic data and structural refinement are listed in Table 3.

Table 3. Crystallographic data and structure refinement for **1** and **2**.

Empirical Formula	$C_{20}H_{16}N_4O_5Cd$	$C_{20}H_{16}N_4O_5Ni$
Formula weight	503.76	451.08
Temperature/K	296(2)	296(2)
Crystal system	Monoclinic	Monoclinic
Space group	*C*2/*c*	$P2_1/c$
a/Å	13.614(5)	14.2023(15)
b/Å	6.270(2)	18.929(2)
c/Å	22.659(8)	7.1289(8)
α/°	90	90
β/°	91.574(6)	94.382(2)
γ/°	90	90
Volume/$Å^3$	1933.4(12)	1910.9(4)
Z	4	4
ρ_{calc}mg/mm^3	1.727	1.568
μ/mm^{-1}	1.171	0.932
F(000)	1000	928
Index ranges	$-16 \le h \le 17$, $-8 \le k \le 8$, $-13 \le l \le 29$	$-18 \le h \le 18$, $-24 \le k \le 23$, $-9 \le l \le 5$
Reflections collected	5530	12981
Independent reflections	2179	4389
Data/restraints/parameters	2179/0/137	4389/0/276
Goodness-of-fit on F^2	1.079	1.034
Final *R* indexes [I> = 2σ (*I*)]	R_1 = 0.0759, wR_2 = 0.2339	R_1 = 0.0253, wR_2 = 0.0648
Final *R* indexes [all data]	R_1 = 0.0808, wR_2 = 0.2419	R_1 = 0.0307, wR_2 = 0.0678
Largest diff. peak/hole / e $Å^{-3}$	2.658/−3.735	0.307 /−0.264

Crystallographic data for the structure reported in this paper has been deposited with the Cambridge Crystallographic Data Centre as supplementary publication Nos. CCDC 1554214 for **1** and 1554215 for **2**. Copy of the data can be obtained free of charge on application to CCDC, 12 Union Road, Cambridge CB2 1EZ, UK (Fax: +44-1223-336-033; E-Mail: deposit@ccdc.cam.ac.uk).

4. Conclusions

In summary, we successfully synthesized two isomers 2-(1*H*-imidazol-4-yl)benzoic acid and 3-(1*H*-imidazol-4-yl)benzoic acid containing 4-imidazolyl and carboxyl functional groups, which were employed to construct two new coordination polymers $[Cd(L_1)_2(H_2O)]_n$ and $[Ni(L_2)_2(H_2O)]_n$. Both of complexes show 2D layer structures, and **1** is a (4, 4) **sql** topology net while **2** is a typical 6^3-**hcb** topology network. Furthermore, complex **1** exhibits blue photoluminescence emission at 455 nm upon excitation at 399 nm.

Acknowledgments: This project was supported by Natural Science Foundation of Fuyang (KJ2011B123).

Author Contributions: Zhu Mei-An, Guo Xing-Zhe and Shi Shan-Shan synthesized the metal coordination polymers. Chen Shui-Sheng designed the method and guided the manuscript.

Conflicts of Interest: The authors declare no conflict of interest.

References

1. Zhao, T.; Heering, C.; Boldog, I.; Domasevitch, K.V.; Janiak, C. A view on systematic truncation of tetrahedral ligands for coordination polymers. *CrystEngComm* **2017**, *19*, 776–780. [CrossRef]
2. Wu, Y.L.; Qian, J.; Yang, G.P.; Yang, F.; Liang, Y.T.; Zhang, W.Y.; Wang, Y.Y. High CO_2 uptake capacity and selectivity in a fascinating nanotube-based metal−organic framework. *Inorg. Chem.* **2017**, *56*, 908–913. [CrossRef] [PubMed]
3. Zhao, D.; Zhang, J.; Yue, D.; Lian, X.; Cui, Y.; Yang, Y.; Qian, G. A highly sensitive near-infrared luminescent metal–organic framework thermometer in the physiological range. *Chem. Commun.* **2016**, *52*, 8259–8262. [CrossRef] [PubMed]
4. Zhao, D.; Cui, Y.; Yang, Y.; Qian, G. Sensing-functional luminescent metal–organic frameworks. *CrystEngComm* **2016**, *18*, 3746–3759. [CrossRef]
5. Zhai, Q.G.; Bu, X.; Mao, C.; Zhao, X.; Feng, P. Systematic and dramatic tuning on gas sorption performance in heterometallic metal−organic frameworks. *J. Am. Chem. Soc.* **2016**, *138*, 2524–2527. [CrossRef] [PubMed]
6. Chen, S.S. The roles of imidazole ligands in coordination supramolecular systems. *CrystEngComm* **2016**, *18*, 6543–6565. [CrossRef]
7. Zeng, W.; Jiang, J. Synthesis and crystal structures of two novel O, N-containing spiro compounds. *Crystals* **2016**, *6*, 69–75. [CrossRef]
8. Chen, S.S.; Sheng, L.Q.; Zhao, Y.; Liu, Z.D.; Qiao, R.; Yang, S. Syntheses, structures, and properties of a series of polyazaheteroaromatic core-based Zn(II) coordination polymers together with carboxylate auxiliary ligands. *Cryst. Growth Des.* **2016**, *16*, 229–241. [CrossRef]
9. Shi, Q.; Xu, W.J.; Huang, R.K.; Zhang, W.X.; Li, Y.; Wang, P.; Shi, F.N.; Li, L.; Li, J.; Dong, J. Zeolite CAN and AFI-type zeolitic imidazolate frameworks with large 12-membered ring pore openings synthesized using bulky amides as structure-directing agents. *J. Am. Chem. Soc.* **2016**, *138*, 2524–2527. [CrossRef] [PubMed]
10. Schmieder, P.; Denysenko, D.; Grzywa Magdysyuk, M.O.; Volkmer, D. A structurally flexible triazolate-based metal–organic framework featuring coordinatively unsaturated copper(I) sites. *Dalton Trans.* **2016**, *45*, 13853–13862. [CrossRef] [PubMed]
11. Nguyen, N.T.T.; Lo, T.N.H.; Kim, J.; Nguyen, HT.D.; Le, T.B.; Cordova, E.; Furukawa, H. Mixed-metal zeolitic imidazolate frameworks and their selective capture of wet carbon dioxide over methane. *Inorg. Chem.* **2016**, *55*, 6201–6207. [CrossRef] [PubMed]
12. Suckert, S.; Germann, L.S.; Dinnebier, R.E.; Werner, J.; Näther, C. Synthesis, structures and properties of cobalt thiocyanate coordination compounds with 4-(hydroxymethyl)pyridine as Co-ligand. *Crystals* **2016**, *6*, 38–54. [CrossRef]
13. Chen, S.S.; Wang, P.; Takamizawa, S.; Okamura, T.A.; Chen, M.; Sun, W.Y. Zinc(II) and cadmium(II) metal-organic frameworks with 4-imidazole containing tripodal ligand: sorption and anion exchange properties. *Dalton Trans.* **2014**, *43*, 6012–6020. [CrossRef] [PubMed]
14. Chen, S.S.; Chen, M.; Takamizawa, S.; Chen, M.S.; Su, Z.; Sun, W.Y. Temperature dependent selective gas sorption of the microporous metal-imidazolate framework [Cu(L)] [H_2L = 1,4-di(1H-imidazol-4-yl) benzene]. *Chem. Commun.* **2011**, *47*, 752–754. [CrossRef] [PubMed]
15. Chen, S.S.; Chen, M.; Takamizawa, S.; Wang, P.; Lv, G.C.; Sun, W.Y. Porous cobalt(II)-imidazolate supramolecular isomeric frameworks with selective gas sorption property. *Chem. Commun.* **2011**, *47*, 4902–4904. [CrossRef] [PubMed]
16. Chen, S.S.; Liu, Q.; Zhao, Y.; Qiao, R.; Sheng, L.Q.; Liu, Z.D.; Yang, S.; Song, C.F. New metal-organic frameworks constructed from the 4-imidazole-carboxylate ligand: structural diversities, luminescence, and gas adsorption properties. *Cryst. Growth Des.* **2014**, *14*, 3727–3741. [CrossRef]
17. Chen, J.; Li, C.P.; Du, M. Substituent effect of R-isophthalates (R = –H, –CH_3, –OCH_3, –tBu, –OH, and –NO_2) on the construction of Cd^{II} coordination polymers incorporating a dipyridyl tecton 2,5-bis(3-pyridyl)-1,3,4-oxadiazole. *CrystEngComm* **2011**, *13*, 1885–1893. [CrossRef]

18. Sheng, Y.W.; Wang, Y.; Okamura, T.A.; Sun, W.Y.; Ueyama, N. Synthesis, crystal structure and nonlinear optical property of cadmium(II) and copper(II) complexes with novel chiral ligand. *Inorg. Chem. Commun.* **2007**, *10*, 432–436. [CrossRef]
19. Guo, X.Z.; Zhang, Z.Y.; Li, Z.L.; Shi, S.S.; Chen, S.S. Synthesis, crystal structures, and properties of two coordination polymers built from imidazolyl and carboxylate ligands. *Crystals* **2017**, *7*, 73. [CrossRef]
20. Kreno, L.E.; Leong, K.; Farha, O.K.; Allendorf, M.; Van Duyne, R.P.; Hupp, J.T. Metal–organic framework materials as chemical sensors. *Chem. Rev.* **2012**, *112*, 1105–1125. [CrossRef] [PubMed]
21. Peng, Y.F.; Zhao, S.; Li, K.; Liu, L.; Li, B.L.; Wu, B. Construction of Cu(II), Zn(II) and Cd(II) metal–organic frameworks of bis(1,2,4-triazol-4-yl)ethane and benzenetricarboxylate: syntheses, structures and photocatalytic properties. *CrystEngComm* **2015**, *17*, 2544–2552. [CrossRef]
22. Sun, Y.X.; Sun, W.Y. Zinc(II)– and cadmium(II)–organic frameworks with 1-imidazole-containing and 1-imidazolecarboxylate ligands. *CrystEngComm* **2015**, *17*, 4045–4063. [CrossRef]
23. Meng, F.; Zhang, M.; Shen, K.; Li, Y.; Zheng, H. A series of MOFs based on a triangular tri(4-pyridylphenyl) amine ligand combined with carboxylate or nitrate auxiliary ligands. *Dalton Trans.* **2015**, *44*, 1412–1419. [CrossRef] [PubMed]
24. Chen, S.S.; Qiao, R.; Sheng, L.Q.; Zhao, Y.; Yang, S.; Chen, M.M.; Liu, Z.D.; Wang, D.H. Cadmium(II) and zinc(II) complexes with rigid 1- (1H-imidazol-4-yl)-3-(4H-tetrazol-5-yl)benzene and varied carboxylate ligands. *CrystEngComm* **2013**, *15*, 5713–5725. [CrossRef]
25. Li, L.N.; Wang, S.Y.; Chen, T.L.; Sun, Z.H.; Luo, J.H.; Hong, M.C. Solvent-dependent formation of Cd(II) coordination polymers based on a C_2-symmetric tricarboxylate linker. *Cryst. Growth Des.* **2012**, *12*, 4109–4115. [CrossRef]
26. Song, S.Y.; Song, X.Z.; Zhao, S.N.; Qin, C.; Su, S.Q.; Zhu, M.; Hao, Z.M.; Zhang, H.J. yntheses, structures and physical properties of transition metal–organic frameworks assembled from trigonal heterofunctional ligands. *Dalton Trans.* **2012**, *41*, 10412–10421. [CrossRef] [PubMed]
27. Sheldrick, G.M. A short history of SHELX. *Acta Cryst.* **2008**, *A64*, 112–122. [CrossRef] [PubMed]